

Phytoremediation-derived sunflower oil for bio-based polyurethane foams

Elżbieta Malewska^{a,b,*}, Jacek Antonkiewicz^c, Maria Kurańska^{a,b}, Piotr Rybarczyk^d, Andrzej Rogala^d

^a Cracow University of Technology, Faculty of Chemical Engineering and Technology, Department of Chemistry and Technology of Polymers, Warszawska 24, Cracow 31-155, Poland

^b Cracow University of Technology, Interdisciplinary Center for Circular Economy, Warszawska 24, Cracow 31-155, Poland

^c University of Agriculture in Krakow, Faculty of Agriculture and Economics, Department of Agricultural and Environmental Chemistry, Mickiewicza 21, Krakow 31-120, Poland

^d Gdansk University of Technology, Faculty of Chemistry, Department of Process Engineering and Chemical Technology, Narutowicza 11/12, Gdansk 80-233, Poland

ARTICLE INFO

Keywords:

Phytoremediation
Transesterification
Biopolyol
Polyurethane
Viscoelastic foams
Insulation foams

ABSTRACT

Sunflowers were planted for phytoextraction of heavy metals from a contaminated effluent-exposed soil substrate. Oil pressed from the sunflower seeds was used as natural, renewable resource for the production of biopolyol and, subsequently, different polyurethane biofoams. The oils were modified via transesterification with triethanolamine (TEA). The biopolyols were characterized using instrumental methods, including FTIR, gel chromatography (GPC), ¹H and ¹³C NMR and MALDI-TOF MS. The biopolyols obtained from remediation (O-R) and commercial (O-C) sunflower oil were characterized by a hydroxyl number above 300 mgKOH/g and a viscosity below 200 mPa·s. Such properties make the biopolyols usable in the production of different types of polyurethane foams, such as open-cell foams for attic insulation and viscoelastic foams intended for pillows or mattresses. The polyurethane foams were subjected to an analysis of their physical and mechanical properties, including apparent density, thermal conductivity, resilience and compressive strength, as well as an investigation of their chemical structure using FTIR and their cellular structure. In addition, it was confirmed that oilseeds from plants used for phytoremediation of degraded soils could be used as a potential source of raw materials for polyurethane chemistry. The resulting biopolyols can replace petrochemical polyol entirely in open-cell insulation foams and up to 20 % in viscoelastic foams.

1. Introduction

One of the top priorities for scientists around the world is to find new sources of renewable raw materials. They are motivated by environmental concerns, finite reserves of petroleum-based raw materials and their unstable prices. The circular economy policy focuses on returning as many by-products and wastes as possible to the raw materials cycle. Many products become waste, but with clever management they can be returned to the raw materials stream (Kara et al., 2022).

The second major challenge is to restore areas that have been degraded by human activities such as industry, coal-based energy production and waste disposal. Contamination of soil and water with heavy metals and hazardous substances remains a global problem. Contamination of the ecosystem is a serious threat to the health of both animals

and humans (Motuzova et al., 2014). In this context, heavy metals are considered the most toxic and dangerous due to their accumulation in soft tissues and the fact they are not metabolized in the human body (Uddin et al., 2021).

Conventional soil treatment systems are very costly and involve depositing contaminated soil in a specific area without providing an immediate solution, but rather postponing the problem. One method of soil and water treatment that is gaining increasing interest is phytoremediation. Phytoremediation is believed to be a new approach to environmental remediation that provides a permanent solution to soil and water contamination problems because it is environmentally friendly, more feasible and affordable (Arthur et al., 2005).

For effective phytoremediation of contaminated land, specially designed plants are planted on the land to absorb contaminants from the

* Corresponding author at: Cracow University of Technology, Faculty of Chemical Engineering and Technology, Department of Chemistry and Technology of Polymers, Warszawska 24, Cracow 31-155, Poland.

E-mail addresses: elzbieta.malewska@pk.edu.pl (E. Malewska), jacek.antonkiewicz@urk.edu.pl (J. Antonkiewicz), maria.kuranska@pk.edu.pl (M. Kurańska), piotr.rybarczyk@pg.edu.pl (P. Rybarczyk), andrzej.rogala@pg.edu.pl (A. Rogala).

<https://doi.org/10.1016/j.indcrop.2025.122439>

Received 11 March 2025; Received in revised form 3 December 2025; Accepted 4 December 2025

Available online 9 December 2025

0926-6690/© 2025 The Authors. Published by Elsevier B.V. This is an open access article under the CC BY license (<http://creativecommons.org/licenses/by/4.0/>).

soil as they grow. The effectiveness of phytoremediation can be surprising because certain groups of plants, known as hyperaccumulators, are resistant to heavy metals. As the name suggests, they have the potential to transport and accumulate soil contaminants up to high concentrations (Adeoye et al., 2022). Another benefit is that the plant roots hold the soil in place, thereby helping to reduce the movement of contaminants deep into the soil, into the groundwater and underground water (Adeoye et al., 2022).

However, phytoremediation also has the critical disadvantage of secondary contamination due to the re-release of heavy metals by plants after phytoremediation. This is because the hyperaccumulating plants only serve as storage containers for the absorbed heavy metals (Tan et al., 2023). The accumulation of large amounts of highly contaminated plant biomass after phytoremediation requires appropriate disposal techniques, and the great majority of solutions to this problem are based on volume-reduction methods such as composting, combustion and gasification (Tan et al., 2023). Conventional volume reduction methods used to treat plant biomass after phytoremediation can not only reduce the entry of harmful contaminants into the food chain, but also convert plant biomass into a form of renewable energy. Thermal degradation processes such as combustion and gasification of plant biomass after phytoremediation can generate thermal and electrical energy (Grifoni et al., 2021). Phytoremediation can also be used to recover metals from plant biomass provided that the metal content is at least 3 % of the dry weight (Kabata-Pendias, 2010).

Another major problem is landfill leachate. If the landfill is inadequately sealed and the hydrological conditions are unfavorable, leachate may migrate to the surrounding arable land, surface water and groundwater, leading to widespread contamination. Contaminants from landfills can be removed using plants with high phytoextraction potential. That purpose can be best fulfilled by using energy crops, including sunflower, and by using the resulting biomass for energy production (Anastopoulos et al., 2021). Urban landfill leachate contains mineral pollutants (e.g. heavy metals, alkaline cations and anions) and organic pollutants (e.g. organic nitrogen compounds, organic acids, hydrocarbons, phenols and detergents), all of which must be recirculated through biological management (Anastopoulos et al., 2021).

Both metallic cations and anions are easily taken up and used in the production of plant biomass. In contrast, high concentrations of heavy metals in the soil environment often inhibit proper plant growth and development (Bashir et al., 2021; Waseem et al., 2024). Therefore, plants that are resistant to metallic contaminants and reduce the toxic effects on plant metabolic processes are recommended (Waseem et al., 2024).

According to the circular economy, combustion should be considered as a last resort, only after all other possibilities for reusing the raw material have been exhausted. Waste burning removes the raw material from the raw material cycle. As reported in the literature, seeds are the part of the plant least capable of absorbing harmful substances. Plants tend to protect their seeds from pollutants. The heavy metal content of various plant organs decreases in the following order: roots > leaves > stem > flowers > seeds (Ociepa-Kubicka and Ociepa, 2012; Dietz and Schnoor, 2001; Yang et al., 2017; Cakaj et al., 2024). Therefore, it makes sense to try to recover at least some of the valuable substances contained in plants, for example, oil extracted from their seeds. The sunflower is one of the oilseed crops whose cultivation enables the efficient phytoextraction of heavy metals from contaminated soil and urban landfill effluent. Sunflowers are characterized by a long growing season, high biomass growth, and high metal uptake from the soil (Qiao et al., 2022). Sunflower and many other oilseed crops are used worldwide to produce so-called biopolyols, which contain at least two hydroxyl groups in the molecule and are used as one of the basic components in the production of polyurethane foams (Tran and Lee, 2023; Sawpan, 2018).

To the best of our knowledge, no studies have yet been published on the potential use of oil extracted from phytoremediation plants in the production of biopolyol dedicated to the synthesis of polyurethane

materials. This paper describes a study in which seeds were harvested from an experimental plot where sunflowers were grown on contaminated soil and irrigated with landfill leachate for phytoremediation. The collected sunflower seeds were pressed to obtain oil, which was then chemically modified and used in the synthesis of two types of polyurethane foams. Commercial sunflowers were used as a reference material.

2. Materials and methods

2.1. Phytoremediation

The research was carried out as part of the BAPR (Baltic Phytoremediation) and ECONUT (Eco-designing for Coastal Zone Nutrients' Circularity) projects. Sunflower is a fast-growing plant that produces seeds and biomass with various potential applications, such as nutritional and energetic use. During its growth, sunflower can also act as a phytoremediation tool, with documented potential for metal phytoextraction from soil. For this reason, the species was selected as the subject of investigation in the BAPR project, where experiments were conducted on post-industrial soil substrates with the aim of soil remediation combined with value-added effects of energetic biomass production. In addition, due to its rapid growth, sunflower is also well suited for testing nutrient uptake from soil within a relatively short period. This characteristic explains its use in the ECONUT project, in which different soil amendments, including those of natural and industrial origin, are being tested. Soil substrates modified with bio-additives were employed in the experiments described in this work. The oil extracted from the harvested sunflower seeds was used to produce biopolyols for the production of polyurethane foams.

Sunflower, of the disease- and pest-resistant variety MAS 83SU, was planted in a field experiment. The growing period of the sunflower lasted from 1 May 2023–30 September 2023. At the end of the sunflower's growing season (150 days), its biomass (above-ground parts) was harvested for energy purposes and oil for the production of polyurethane foams. During vegetation, the sunflower was watered with industrial effluent from a communal landfill. For the first two weeks of the experiment, sunflower seedlings were watered exclusively with distilled water to acclimatize the plant to the growing conditions. After two weeks, during the growing season, the plants were watered daily with distilled water and once a week with wastewater, maintaining soil moisture at 60 % of the maximum water capacity. The wastewater used for plant irrigation was collected from a landfill leachate collection point as a concentrate after reverse osmosis treatment. In accordance with the legislation, there were no exceedances of the permissible values of the pollutant indicators entering the industrial sewage systems (Parliament of the Republic of Poland 2020).

The chemical composition of the leachate used to water the sunflowers is shown in Table 1. The leachate from the municipal landfill was rich in mineral and organic components making it a source of essential (nutrients) and non-essential substances for the remediation plants.

Table 2 shows the analysis results regarding the heavy metal content of the sunflower seeds obtained through phytoremediation, commercial sunflower seeds, and the soil in which the sunflowers were grown. The mineralization of soil and sunflower seed samples was performed using a Multiwave 5000 microwave digestion system (Anton Paar) equipped with a Rotor 41HVT56. The mineralization of soil samples was performed using a mixture of concentrated HCl (35–38 %) and HNO₃ (65 %) (3:1 v/v, inverse aqua regia), while sunflower seed samples were mineralized with a mixture of HNO₃ (65 %) and H₂O₂ (30 %, hydrogen peroxide) (7:1 v/v), in accordance with ISO 11466:2002 and PN-R-04014:1991. Elemental determination in the mineralized soil and sunflower seed samples was carried out using inductively coupled plasma optical emission spectrometry (ICP-OES, OPTIMA 7300 DV, PerkinElmer, Waltham, MA, USA). For quality control, the standard reference material ISE 953 (WEPAL-QUASIMEME, International Plant-Analytical

Table 1

Selected parameters of wastewaters (based on Annual Environmental Monitoring Report for Landfill at the Municipal Waste Rendering Plant in Gdańsk, 2023).

| Parameter | Unit | Value |
|---|----------------------|---------------|
| pH | | 6.7 ± 0.2* |
| Electrical conductivity | μS•cm ⁻¹ | 38000 ± 120 |
| Turbidity | NTU | 895 ± 10 |
| Odor | TON | > 1000 ± 10 |
| Suspensions | mg•L ⁻¹ | 1790 ± 36 |
| Dissolved substances | mg•L ⁻¹ | 37630 ± 40 |
| Dry residue | mg•L ⁻¹ | 39400 ± 80 |
| Biochemical oxygen demand (BOD ₅) | mg•L ⁻¹ | 17050 ± 40 |
| Chemical oxygen demand (COD _{Cr}) | mg•L ⁻¹ | 34800 ± 56 |
| Permanganate index | mg•L ⁻¹ | 2360 ± 45 |
| Ammonium nitrogen | mg•L ⁻¹ | 3120 ± 64 |
| Nitrate nitrogen | mg•L ⁻¹ | 1.81 ± 0.10 |
| Total nitrogen | mg•L ⁻¹ | 3355 ± 30 |
| Chlorides | mg•L ⁻¹ | 8340 ± 105 |
| Sulfates | mg•L ⁻¹ | 11500 ± 235 |
| Fluorides | mg•L ⁻¹ | 1630 ± 20 |
| Phosphates | mg•L ⁻¹ | 329 ± 24 |
| Sulfides | mg•L ⁻¹ | 34.6 ± 4.8 |
| Phenol index | mg•L ⁻¹ | 3.35 ± 0.05 |
| Substance extractable with petroleum ether | mg•L ⁻¹ | 290 ± 8 |
| Copper (Cu) | mg•L ⁻¹ | 0.184 ± 0.02 |
| Zinc (Zn) | mg•L ⁻¹ | 6.11 ± 0.05 |
| Lead (Pb) | mg•L ⁻¹ | < 0.010 |
| Cadmium (Cd) | mg•L ⁻¹ | < 0.005 |
| Chromium (VI) | mg•L ⁻¹ | < 0.010 |
| Chromium – Total (Cr) | mg•L ⁻¹ | 1.56 ± 0.05 |
| Nickel (Ni) | mg•L ⁻¹ | 0.87 ± 0.04 |
| Iron – Total (Fe) | mg•L ⁻¹ | 41.2 ± 0.4 |
| Manganese (Mn) | mg•L ⁻¹ | 13.8 ± 1.1 |
| Mercury (Hg) | mg•L ⁻¹ | < 0.0005 |
| Potassium (K) | mg•L ⁻¹ | 2960 ± 36 |
| Sodium (Na) | mg•L ⁻¹ | 2654 ± 16 |
| Calcium (Ca) | mg•L ⁻¹ | 1790 ± 24 |
| Magnesium (Mg) | mg•L ⁻¹ | 357 ± 1 |
| General hardness | mmol•L ⁻¹ | 65.4 ± 4.5 |
| Polycyclic aromatic hydrocarbons (PAHs) | μg•L ⁻¹ | 0.059 ± 0.005 |
| Total organic carbon (TOC) | mg•L ⁻¹ | 10750 ± 50 |

Table 2

Heavy metal content in soil and sunflower seeds.

| Object / Metal | Zn mg•kg ⁻¹ d.m. | Cu | Ni | Cr | Cd | Pb |
|-----------------------------------|--------------------------------|-------------|-------------|-------------|-------------|-------------|
| Soil | 135.2 ± 8.5 | 38.4 ± 2.8 | 18.5 ± 1.2 | 36.0 ± 3.4 | 1.6 ± 0.4 | 32.6 ± 3.1 |
| Phytoremediation sunflowers seeds | 24.65 ± 1.90 | 2.51 ± 0.13 | 1.56 ± 0.11 | 0.86 ± 0.07 | 0.24 ± 0.02 | 2.13 ± 0.15 |
| Commercial sunflowers seeds | 11.55 ± 1.36 | 2.24 ± 0.11 | 1.26 ± 0.14 | 0.57 ± 0.09 | 0.11 ± 0.03 | 1.84 ± 0.12 |

Exchange, Wageningen, The Netherlands) was used. Recovery values ranged from 88 % to 106 %, which were considered satisfactory. The results suggest that this raw material is safe to use in the production of biopolyols and foam. Based on chemical analysis, the content of Zn, Cu, and Cd in the soil, where the field experiment was conducted, indicated grade I soil contamination (Kabata-Pendias et al., 1993). However, the level of heavy metals in the sunflower seeds, as a result of the remediation process, did not exceed the permissible levels for plants intended for use as animal fodder (Kabata-Pendias et al., 1993).

2.2. Synthesis of biopolyols

Oil pressed from commercial sunflower seeds (C-O) and oil from phytoremediation (R-O) were used to synthesise biopolyols. The oil pressing yields were 28 and 41 %, respectively. Sunflower seeds obtained from the conducted phytoremediation process and commercial sunflower seeds were used in the study. Fig. 1 presents the appearance of the seeds.

Sunflower oils were chemically modified by transesterifying. The reaction conditions were selected on the basis of previous studies concerning other oils, i.e. cooking oil or oilseed radish oil (Kurańska and Malewska, 2021; Malewska et al., 2024a). For the transesterification of the triacylglycerols (TG, also known as triglycerides), pure triethanolamine (TEA) was used as the transesterification agent and anhydrous zinc acetate as the catalyst. Chempur Poland supplied both reagents. A glass reactor (volume: 500 mL) equipped with a mechanical stirrer and a reflux condenser was used for the transesterification reaction. The reactor contained the 200 g of oil, the transesterification agent and the catalyst. The mole ratio of oil to TEA was 1:3 (considering the molecular weight of the oils as determined by GPC). The catalyst was added at 0.3 % of the total weight of oil and TEA. All components were heated to 175°C. The mixture was stirred at 400 rpm. The reaction was allowed to run for 2 h. The mixture obtained after the reaction was cooled down and then analyzed. Two biopolyols were obtained: one from commercial sunflower oil (BP-C), and one from phytoremediated sunflower oil (BP-R). The biopolyols were used for the synthesis of different types of polyurethane foams (PUFs) without any further purification or separation processes.



Fig. 1. Sunflower seeds (a) obtained from a phytoremediation process; (b) commercial.

Oils and biopolyols were characterised by the following methods:

- According to the PN-C-89052-03:1993 standard, the hydroxyl value (OH_{val}) was determined.
- The Karl Fisher method according to PN-81/C-04959 was used to determine the water content ($\%\text{H}_2\text{O}$).
- Viscosity was determined using a Lamy Rheology CP-4000 at 25 °C.
- Gel permeation chromatography (GPC) analysis was used to determine the number average molecular weight (M_n). A Knauer chromatograph equipped with a PLgel MIXED-E column for the analysis of oligomers and a refractive-index (RI) detector was used. THF (HPLC grade) was used as the mobile phase at a flow rate of 0.5 mL min⁻¹ and a column temperature of 35 °C. Note: under the present conditions, highly polar, low-molecular-weight species (e.g., glycerol (GLY)) exhibit limited solubility and a low RI response and may not elute quantitatively. Consequently, they are not included in the reported M_n .
- The chemical structures were analysed using an FTIR spectrometer model Nicolet iS5 from Thermo Fisher Scientific (Waltham, MA, USA), equipped with an ATR (attenuated total reflection) accessory with a diamond crystal in the infrared range of 4000–500 cm⁻¹.
- MALDI-TOF mass spectra were acquired using the UltrafleXtreme TOF/TOF mass spectrometer (Bruker Daltonics, Bremen, Germany) equipped with a smartbeam-II 355 nm laser operated at 2000 Hz in positive-ion reflection mode. Panoramic pulsed ion extraction and external calibration were used for accurate mass assignment. Samples were prepared by the dried-droplet method: solution of the sample (10 mg mL⁻¹), the matrix 2,5-Dihydroxybenzoic acid (DHB, Sigma-Aldrich, 98 %, 20 mg mL⁻¹), and the ionizing agent sodium trifluoroacetate (NaTFA; Sigma-Aldrich, 10 mg mL⁻¹) in THF (Sigma-Aldrich, anhydrous, 99.9 %) were mixed in a volume ratio 4:20:1. 1 µL of the mixture was deposited on a ground steel target.
- ¹H (400.1 MHz) and ¹³C (100.6 MHz) NMR spectra were recorded on a Bruker Avance 400 spectrometer at 298 K in CHCl₃ (chemical-shift references: $\delta_{\text{H}} = 7.26$ ppm, $\delta_{\text{C}} = 77.16$ ppm). For ¹H NMR, a 90° pulse of 16.5 µs, recycle delay $d_1 = 10$ s, and 32 scans were used to obtain quantitative integrals. For ¹³C NMR, a 90° pulse of 10 µs, $d_1 = 10$ s, and 4096 scans were employed.

NMR analysis was used to confirm the chemical structures of the vegetable oils and the TEA-based biopolyols. Based on the quantitative ¹H NMR, the average number of free-OH groups per TEA molecule (f_{NMR}) in the TEA-based biopolyols mixture (TEA- mono-, di-, tri-esters and unreacted TEA, excluding the GLY formed during transesterification) was calculated from the methylene signals adjacent to oxygen (OCH₂). The integral of free-arm OCH₂ (-O-CH₂-CH₂-OH), δ 3.50–3.75 ppm) is denoted I_{free} and the integral of esterified-arm OCH₂ (-O-CH₂-C(O)-R, δ 4.05–4.35 ppm) is denoted I_{ester} . The hydroxyl functionality were calculated as:

$$f_{\text{NMR}} = 3 \frac{I_{\text{free}}}{I_{\text{free}} - I_{\text{ester}}}$$

2.3. Preparation of viscoelastic foams

3 different petrochemical polyether polyols were used to produce viscoelastic polyurethane foams (VPUF):

- Polyol 1 - polyoxyalkylene multihydroxyls alcohol; $\text{OH}_{\text{val}} = 410$ mgKOH/g; $M_n \sim 600$ g/mol; $\%\text{H}_2\text{O} = 0.1$ %,
- Polyol 2 - GLY-based copolymer block-statistic on ethylene oxide and propylene oxide; $\text{OH}_{\text{val}} = 33$ mgKOH/g; $M_n \sim 5000$ g/mol; $\%\text{H}_2\text{O} = 0.1$ %,

- Polyol 3 - GLY-based reactive polyoxyalkylene triol; $\text{OH}_{\text{val}} = 28$ mgKOH/g; $M_n \sim 6000$ g/mol; $\%\text{H}_2\text{O} = 0.1$ %) and the biopolyols from sunflower oil.

The PUR system also contains:

- catalyst DABCO NE600 supplied by Evonik Industries AG,
- surfactant NIAx® SILICONE L-618 supplied by Momentive Performance Materials Inc.,
- water as a chemical foaming agent,
- chain extender: 1,3-butanediol (pure for analysis) supplied by Sigma-Aldrich Products,
- isocyanate Ongronat® 3800 supplied by BorsodChem, Hungary.

Table 3 shows the formulations used to obtain the VPUF. The amount of isocyanate, taking into account the hydroxyl number and water content of the polyol components, was calculated separately for each system in order to keep the isocyanate index the same for all formulations. Isocyanate index is the ratio of isocyanate groups to the number of reactive hydrogen atoms in the polyol. It is usually expressed as a percentage. A reference foam was prepared. This contained only petrochemical polyols. The reference foam was then modified by replacing 20 % of the petrochemical polyols with the synthesised bio-polyol. For this purpose, 10 % of polyol 1 and 10 % of polyol 3 were replaced by the newly obtained biopolyol.

Under laboratory conditions, the foamed PUR materials were prepared. Firstly, a polyol premix was prepared by mixing all components except isocyanate for 30 s. An appropriate amount of isocyanate was added to the polyol premix and mixed for 8 s. The mixture was poured into a mold where the foam was allowed to grow free. The foam was aged for 3 days.

Viscoelastic foam samples were subjected to the following tests:

- The ISO 845:2006 standard was used to calculate the apparent density of the foams.
- The morphology of cells was analysed using a scanning electron microscope (Hitachi TM3000). The analysis of the foam morphology (cell cross-section area and number of cell per mm²) was performed using ImageJ software (U.S. National Institutes of Health, Bethesda, MD, USA).
- The compressive strength was measured using a Zwick Z005 TH Allround-Line in accordance with the PN-EN ISO 3386-1:1997 standard. Based on these results, hysteresis loop plots of compressive stress were obtained. Hysteresis, support factor, compressive stress at 75 % deformation and hardness (strain at 40 % deformation) were determined.
- The steel ball method was used to measure foam resilience in a direction parallel to the direction of foam growth, in accordance with ISO 8307:2007.
- Foam return time was measured according to the IKEA IOS-MAT-0076 standard.

Table 3

The formulations of viscoelastic polyurethane foams.

| Components, g | | Foam symbol | | |
|------------------|------|-------------|----------|----------|
| | | VPU-REF | VPU-BP-C | VPU-BP-R |
| Biopolyols | BP-C | - | 20 | - |
| | BP-R | - | - | 20 |
| Polyol 1 | | 40 | 30 | 30 |
| Polyol 2 | | 20 | 20 | 20 |
| Polyol 3 | | 40 | 30 | 30 |
| Catalyst | | 1.0 | 1.0 | 1.0 |
| Surfactant | | 1.2 | 1.2 | 1.2 |
| H ₂ O | | 2.5 | 2.5 | 2.5 |
| Chain Extender | | 3.0 | 3.0 | 3.0 |
| Index NCO, % | | 55 | 55 | 55 |

2.4. Preparation of thermal insulation polyurethane foams

Open-cell reference foams (OPU-REF) were obtained using petrochemical polyether polyols (Polyol 1), whereas open-cell biofoams (OPU-BP-C and OPU-BP-R) were obtained using the biopolyols from sunflower oils.

The PUR systems included also:

- catalysts Kosmos 19, Polycat 15 and PC Cat NP110 supplied by Evonik Industries AG, Germany,
- surfactant Tegostab B8870, Ortegol 500 supplied by Evonik Industries AG, Germany,
- water as a chemical foaming agent,
- isocyanate Ongronat®2100 supplied by BorsodChem, Hungary.

The formulations used are shown in Table 4. The amount of isocyanate, taking into account the hydroxyl number and water content of the polyol components, was calculated separately for each system in order to keep the isocyanate index the same for all formulations. The reference foam was modified by replacing 100 % of the petrochemical polyols with the synthesized biopolyol.

Open-cell foam samples were subjected to the following tests:

- The ISO4590:2016 standard was used to measure the closed cell content of the foams.
- The thermal conductivity coefficient was measured according to ISO 8301 using a Fox200 heat flow meter (TA Instruments, DE, USA) at an average temperature of 10°C.
- The apparent density was measured in accordance with the ISO 845:2006 standard.
- Compressive strength measurements were carried out according to EN ISO 844:2021. The samples were tested in parallel and perpendicular directions to foam growth using a Zwick Roell testing machine.

3. Results and discussion

3.1. Biopolyols

Sunflower seeds used for polyol synthesis were obtained from sunflowers grown under standard cultivation conditions as well as from those employed in phytoremediation. Based on the scientific literature, it can be inferred that the fatty acid profile of sunflower oil typically consists of linoleic acid as the predominant component (~58 %), followed by oleic acid (~28 %), with lower amounts of palmitic (~7 %) and stearic acids (~3 %), and only trace levels of α -linolenic acid (~0.1 %) (Nakonechna et al., 2024). Therefore, the resulting biopolyol will be a mixture of compounds containing various fatty acyl moieties derived from these fatty acids. A transesterification reaction was carried out to introduce hydroxyl groups into the oil, with TEA as the transesterification agent. The research plan assumed that a biopolyol with a functionality close to 2 would be needed to secure the possibility of producing various polyurethane materials. A trifunctional

transesterification agent can be used for this purpose. The most commonly available agents of this type are TEA and glycerol (GLY). However, GLY reacts slower and requires higher temperatures (250°C) than TEA (175°C) (Fridrihsone-Girone and Stirna, 2014; Kurańska and Malewska, 2021).

Fig. 2 presents the appearance of fresh oils (Fig. 2a-b) and the biopolyols obtained with their participation (Fig. 2c-d). As a result of transesterification, the oils extracted from sunflower seeds changed color from light yellow to dark brown.

According to the literature, the transesterification of oils with polyhydric alcohols is a reversible process that proceeds in successive stages, accompanied by the formation of intermediate products. Consequently, a detailed structural characterization of the obtained biopolyol, which represents a complex mixture of several compounds containing different fatty acyl moieties, was required. To achieve this, FTIR NMR, and MALDI-TOF MS were employed.

Fig. 3 shows the FTIR spectra of oils and the obtained biopolyols. The spectra confirm that there are no differences in the chemical structure between commercial sunflower oil and sunflower oil derived from phytoremediation. An analogous situation was observed in the spectra of the biopolyols. Based on the FTIR spectra for oils (lower spectrum) and biopolyols (upper spectrum), the following characteristic bands can be identified. In the oils, characteristic absorption bands were detected: ~3005–2850 cm^{-1} – strong C–H stretching bands ($-\text{CH}_2-$, $-\text{CH}_3$) characteristic of aliphatic fatty acyl chains; ~1740 cm^{-1} – intense carbonyl ($\text{C}=\text{O}$) stretching band typical of esters (main feature of triglycerides); ~1465 and 1375 cm^{-1} – deformation vibrations of CH_2 and CH_3 groups; ~1160–1090 cm^{-1} – C–O stretching bands in ester linkages. In the case of biopolyols, the following bands were observed: ~3400–3200 cm^{-1} – broad O–H stretching band, appearing in biopolyols as a result of transesterification and the formation of hydroxyl groups; ~3000–2850 cm^{-1} – aliphatic C–H bands of fatty acyl chains, similar to those in oils; ~1740 cm^{-1} – $\text{C}=\text{O}$ stretching band from ester residues, often with altered intensity compared to oils, depending on the degree of modification; ~1200–1000 cm^{-1} – increased intensity in the region of C–O–C and C–O vibrations, related to the presence of new hydroxyl and alkoxy groups in biopolyols; ~1465 and 1375 cm^{-1} – CH_2/CH_3 deformations, similar to oils.

The ^1H NMR spectra of sunflower oils (O-C, O-R, Fig. 4a and b) are consistent with triacylglycerols (TG), as described in the literature (Di Pietro et al., 2020; Alexandri et al., 2017), and all expected resonances were assigned as follows: terminal CH_3 at δ 0.80–0.85 (t, A); aliphatic (CH_2) at δ 1.15–1.35 (br m, B); β - CH_2 to carbonyl ($-\text{CH}_2-\text{CH}_2-\text{C}(=\text{O})-$) at δ 1.50–1.60 (m, C); allylic CH_2 ($-\text{CH}_2-\text{CH}=\text{CH}-$) at δ 1.90–2.05 (m, D); α - CH_2 to $\text{C}=\text{O}$ ($-\text{CH}_2-\text{C}(=\text{O})-\text{O}-$) at δ 2.20–2.30 (t, E); bis-allylic CH_2 ($-\text{CH}=\text{CH}-\text{CH}_2-\text{CH}=\text{CH}-$) at δ 2.65–2.75 (m, F); sn-1,3 $\text{CH}_2-\text{O}-\text{CO}$ at δ 4.00–4.30 (m, G); sn-2 $\text{CH}-\text{O}-\text{CO}$ at δ 5.15–5.23 (m, H); olefinic $=\text{CH}-$ at δ 5.25–5.35 (m, I). In the TEA-based biopolyols (BP-C, BP-R, Fig. 4) new signals are observed (Mondal and Pratap, 2016): NCH_2 ($-\text{CH}_2-\text{N} <$) at δ 2.52–2.60 and 2.62–2.67 (m, J, shifts to higher ppm with increasing degree of esterification and overlap with the bis-allylic $-\text{CH}_2-$ at 2.65–2.75); NCH_2 of esterified arms ($-\text{CH}_2-\text{CH}_2-\text{OCO}-$) at δ 2.72–2.78 (m, K); OCH_2 of free TEA arms ($-\text{O}-\text{CH}_2-\text{CH}_2-\text{OH}$) at δ 3.50–3.70 (m, L); OCH_2 of esterified arms ($-\text{O}-\text{CH}_2-\text{C}(\text{O})-\text{R}$) at δ 4.00–4.20 (m, M). The sum of the integrals for TEA NCH_2 (J+K) and OCH_2 (L+M) is consistent with the expected 6:6 (1:1) proton ratio and supports the assignments.

Upon transesterification with TEA, the biopolyol spectra (BP-C, BP-R, Fig. 4c and d) show disappearance/strong attenuation of the TG signals H and G, which confirms complete conversion of TG to TEA esters. The aliphatic (signals A-E) and unsaturated regions (F and I) are retained, indicating that hydrocarbon chains and $\text{C}=\text{C}$ bonds remain unmodified. Using the quantitative OCH_2 integrals defined in Methods, the hydroxyl functionality (f_{NMR}) of the TEA-based biopolyol mixture was obtained and is reported in Table 6. The values of $f_{\text{NMR}} = 2.03 \pm 0.10$ for BP-C and 1.94 ± 0.04 for BP-R (the uncertainty from integration-window and baseline variation). ^{13}C NMR spectra were

Table 4
The formulations of open-cell polyurethane foams.

| Components, g | | Foam symbol | | |
|------------------|------|-------------|----------|----------|
| | | OPU-REF | OPU-BP-C | OPU-BP-R |
| Biopolyols | BP-C | - | 100 | - |
| | BP-R | - | - | 100 |
| Polyol 1 | | 100 | - | - |
| Catalyst | | 3.7 | 3.7 | 3.7 |
| Surfactant | | 5.5 | 5.5 | 5.5 |
| H ₂ O | | 15 | 15 | 15 |
| Index NCO | | 110 | 110 | 110 |

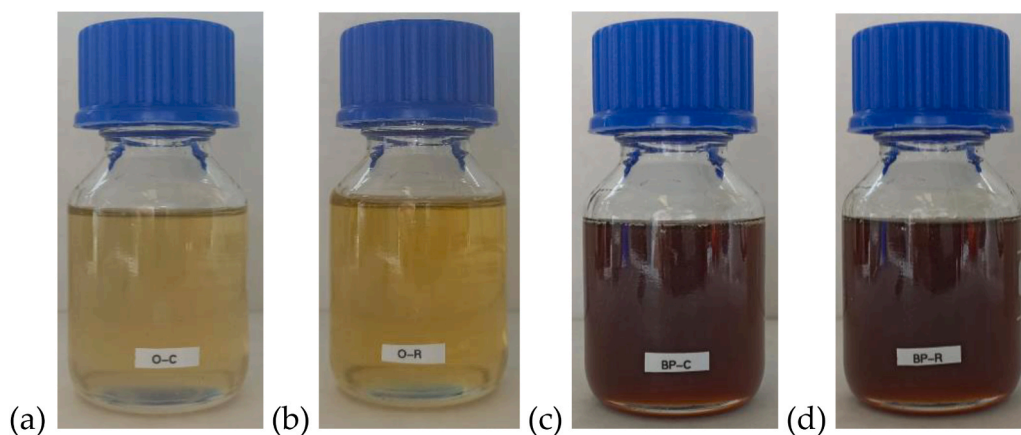


Fig. 2. Appearance of (a) O-C; (b) O-R; (c) BP-C; (d) BP-R.

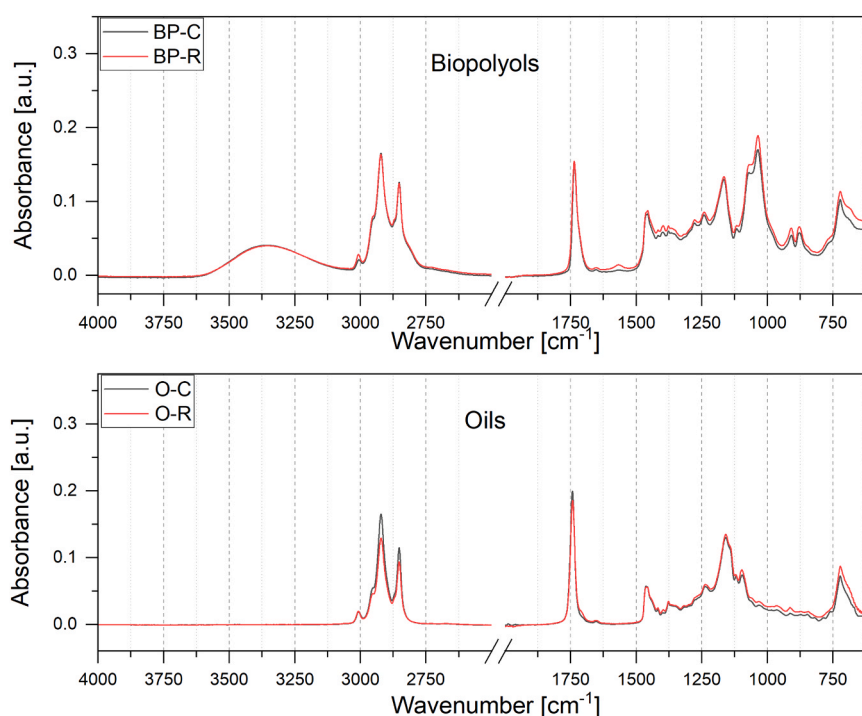


Fig. 3. FTIR spectra of oils and biopolyols.

acquired and selected signals assigned to the structure of the products. For the oils (O-C, O-R), the GLY backbone was assigned as sn-1,3 CH₂-O-CO at $\delta \sim 62$ ppm (a) and sn-2 CH-O-CO at $\delta \sim 69$ ppm (b). In the biopolyols (BP-C, BP-R, Fig. 4) NCH₂ appears at $\delta \sim 53$ (c) and a more deshielded NCH₂ at $\delta \sim 56.5$ (d); OCH₂ of free TEA arms (-O-CH₂-CH₂-OH) at $\delta \sim 59.0$ (e); OCH₂ adjacent to the ester group (-O-CH₂-C(O)-R) at $\delta \sim 61.8$ (f). A minor overlap with signal f with residual GLY near ~ 62 ppm can occur, however, the disappearance of the GLY signals in ¹H NMR (sn-2 at 5.20–5.30 ppm) indicates that the 61–62 ppm signal in BP-C and BP-R samples is dominated by TEA OCH₂-CO.

In line with the NMR assignment, MALDI-TOF mass spectrometry (shown in Fig. 5) was used to further confirmed the formation of TEA mono-, di-, and tri-esters. Using NaTFA as the cationizing agent, the spectra displayed the expected cationized adducts. The comprehensive list in Table 5 confirms the presence of acyl residues derived from palmitic (C16:0), oleic (C18:1), linoleic (C18:2), and linolenic (C18:3) acids. Within each homologous series, adjacent members differing by

one C=C show the characteristic ~ 2.016 Da spacing (mass change corresponding to 2 H), consistent with the distribution of unsaturations in sunflower oil. Because the samples contained measurable amounts of K⁺ ions, each molecular species appeared as a [M+Na]⁺ and [M+K]⁺ pair ($\Delta m \approx 15.97$ Da). Weak [M+H]⁺ ions were also observed.

In the TEA-based biopolyols (BP-C, BP-R), the spectra show cationized adducts of TEA mono-, di-, and tri-esters. Notably, no signals attributed to residual glycerol esters (Triacylglycerol-TG/Diacylglycerol-DG/Monoacylglycerol-MG) were detected, which together with NMR confirms complete conversion of the starting TG into TEA esters.

Based on a review of the literature and the analyses performed, the following reaction schemes illustrate the formation of TEA-based polyol (Fig. 6).

During the transesterification of triacylglycerols (TG) with triethanolamine (TEA), the process proceeds stepwise. In the initial stage, one fatty acyl group from a TG is transferred to TEA, yielding a TEA monoester and a diacylglycerol (DG). In the next stage, DG undergoes an

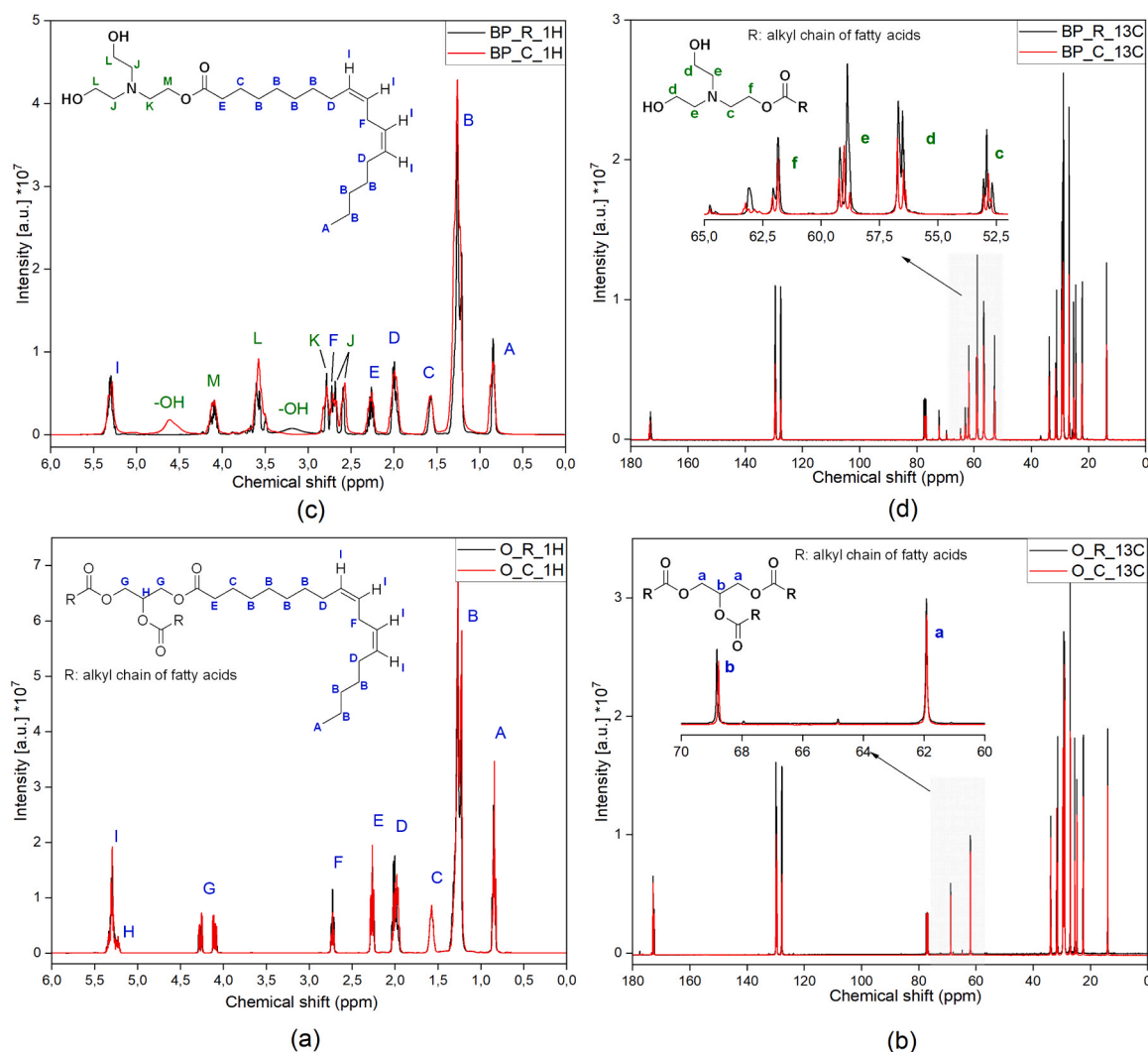


Fig. 4. NMR spectra: (a) ^1H and (b) ^{13}C spectra of the oils (O-C, O-R); (c) ^1H and (d) ^{13}C spectra of the TEA biopolyols.

analogous transfer, forming a second TEA monoester and a monoacylglycerol (MG). Finally, the MG reacts with TEA to release glycerol (GLY) and another TEA monoester. In parallel with this main sequence, competitive transesterifications can further acylate the TEA monoester to the TEA diester (via reaction with TG, DG or MG) and, upon subsequent acyl transfer, to the TEA triester.

In the subsequent stages of the study, the physicochemical properties of sunflower oils and the biopolyols obtained from them were analyzed, with particular emphasis on the characteristics relevant for assessing their suitability for polyurethane synthesis. The results of the hydroxyl value, molecular weight, viscosity, water content, and functionality determinations are summarized in Table 6.

The analyses show that the commercial and remediation-sourced oils have similar average molar masses ranging from 880 to 890 g/mol. Similar results have been reported in the literature for sunflower oils (Cuevas et al., 2009). The water content is also comparable across the analyzed oils, ranging from 0.12 % to 0.14 %.

Two different products were obtained by performing the transesterification reaction of sunflower oils with TEA. The products were homogeneous and did not stratify. The biopolyols were characterized by a lower average molar mass compared to the initial oil (500 g/mol for BP-C and BP-R), indicating that the transesterification process occurred. Bearing in mind the intended application of the hydroxyl derivatives in the production of polyurethane materials, it was necessary to determine the value of the hydroxyl number. The hydroxyl number of the

biopolyols was found to be about 330 mgKOH/g (329 mgKOH/g for BP-C and 337 mgKOH/g for BP-R). The difference in hydroxyl value between the biopolyols obtained at 8 mg KOH/g is negligible, falling within the margin of error, and only slightly affects the amount of isocyanate added to the polyurethane reaction. Stirna et al. also used TEA in transesterification to obtain sunflower oil-based biopolyol characterized by a hydroxyl number of 310 mg KOH/g (Stirna et al., 2008). Previous studies in which biopolyols were produced using the same method and TEA but with different starting oils gave biopolyols with the following hydroxyl values: from rapeseed oil - $\text{OH}_{\text{val}} = 374$ mgKOH/g (Stirna et al., 2013); from waste cooking oil - $\text{OH}_{\text{val}} = 348$ mgKOH/g (Kurańska et al., 2020); from oilseed radish oil - $\text{OH}_{\text{val}} = 346$ mgKOH/g (Malewska et al., 2024a).

The viscosities of the biopolyols obtained were 170 mPa·s and 160 mPa·s for BP-C and BP-R, respectively. While the viscosities increased in relation to those of the initial oils, they remain relatively low compared to other polyols. For example, biopolyols produced by epoxidation of double bonds and opening of oxirane rings had viscosities from 6000 mPa·s (Borowicz et al., 2025) to about 60,000 mPa·s or more (Ionescu and Petrović, 2010). The viscosities of typical commercial petrochemical polyols are also significantly higher. The viscosities of polyether polyols range from 2000 to 14,000 mPa·s (Ionescu and Petrović, 2010). From a processing point of view, the viscosity value of the raw materials used to produce polyurethane is important. If the viscosity is too high, it may affect the efficiency of dosing and mixing substrates, as well as the

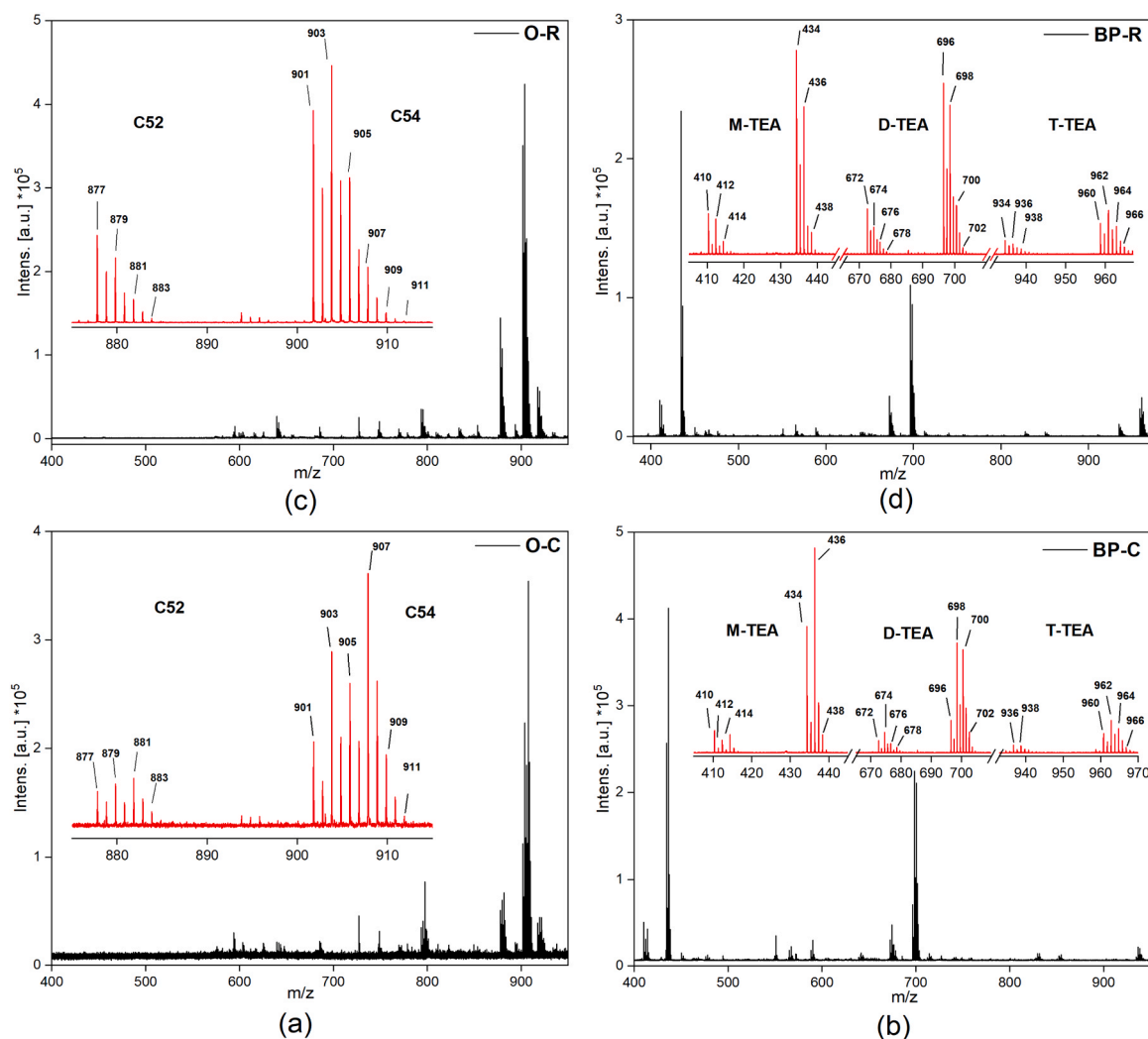


Fig. 5. MALDI-TOF mass spectra: (a) oil O-C; (b) biopolyol BP-C; (c) oil O-R; (d) biopolyol BP-R.

cellular structure formed. The water content in biopolyols is essential during the formulation of polyurethane biofoams. content in the obtained biopolyols was about 0.3 %.

The transesterification reaction results in a product that is a mixture of several components. Depending on the selected reaction conditions, different reaction yields can be achieved (Keera et al., 2011). As a result of the reaction of vegetable oil with TEA containing three hydroxyl groups, a mixture of TEA esters is produced (Stirna et al., 2013; Malewska et al., 2022; da Silva et al., 2015). The presence of various compounds in the reaction mixture is also confirmed by GPC analysis. Fig. 7 presents a comparison of chromatograms for the starting oils and the products of the transesterification process. Fig. 7a shows that for the starting oils, there is only one peak in the chromatogram around 16th minute corresponding to the presence of TG. The chromatogram shown in Fig. 7b was obtained during the analysis of the TEA-based biopolyols and looks different. The first peak also appears at the 16th minute but corresponds to the presence of TEA-triesters, as indicated by the average molecular weight determined by GPC. The next two peaks appearing in the chromatogram at 17th and 18th minute testify to the presence of TEA-diester and TEA-monoester, respectively. The surface areas of these peaks are significantly larger.

Table 7 presents the percentage areas of individual peaks along with their corresponding average molar masses. The content of TEA-triesters is relatively low, at approximately 9 % for both polyols. TEA-diester constitute roughly 37 % of the total, whereas the predominant

products, TEA-monoesters, represent around 50 %. The final peak, appearing at the 21st minute with a percentage area of approximately 4 %, corresponds to unreacted TEA, as indicated by its molecular weight.

3.2. Application of biopolyols in polyurethane synthesis

The biopolyols obtained from commercial and remediated sunflower had similar physico-chemical properties, so it was decided to synthesize polyurethane foams using both biopolyols. Polyols obtained on an industrial scale can exhibit a very wide range of properties. Hydroxyl values range from 20 to 500 mgKOH/g. Polyols also vary in viscosity and molar mass, which are important factors to consider when working with these substances. This variation is intentional, as different polyurethanes with different physical and mechanical properties are obtained depending on the properties of the polyol used for different applications. A decision was made to obtain two types of polyurethane foams in the synthesis of which a biopolyol with such a high hydroxyl value could be used, i.e. for thermal insulation open-cell polyurethane foams and for viscoelastic foams. Both foams produced contain open cells. To obtain such a structure, an appropriate combination of catalysts, surfactants, and foaming agents must be employed so that, during foam formation, the pressure generated inside the cells ruptures the cell walls and allows the blowing agent to escape. This process must be synchronized with the gelation of the forming polyurethane to prevent

Table 5

Summary of MALDI-TOF mass signals assigned to triacylglycerols and TEA esters.

| m/z^a [Da] | Identification ^c |
|--|------------------------------------|
| Sunflower oil (O-C and O-R) (peaks marked in red in Fig. 5a and c) | |
| 877 | [C52:4] (PLL) TG |
| 879 | [C52:3] (POL) |
| 881 | [C52:2] (POO) |
| 883 | [C52:1] (PSO) |
| 901 | [C54:6] (LLL) |
| 903 | [C54:5] (OLL) |
| 905 | [C54:4] (OOL) |
| 907 | [C54:3] (OOO) |
| 909 | [C54:2] (SOO) |
| 911 | [C54:1] (SSO) |
| Sunflower-oil biopolyol (BP-C and BP-R) (peaks marked in red in Fig. 5b and d) | |
| 410 | [C16:0] (P) TEA-M (TEA-monoester) |
| 412 ^b | [C18:2] (L) |
| 414 ^b | [C18:1] (O) |
| 434 | [C18:2] (L) |
| 436 | [C18:1] (O) |
| 438 | [C18:0] (S) |
| 672 | [C34:2] (PL) TEA-D (TEA-diester) |
| 674 | [C34:1] (PO) |
| 676 | [C34:0] (PS) |
| 696 | [C36:4] (LL) |
| 698 | [C34:3] (OL) |
| 700 | [C34:2] (OO) |
| 702 | [C34:1] (OS) |
| 936 | [C52:3] (POL) TEA-T (TEA-triester) |
| 938 | [C52:2] (POO) |
| 960 | [C54:5] (OLL) |
| 962 | [C54:4] (OOL) |
| 964 | [C54:3] (OOO) |
| 966 | [C54:2] (SOO) |

^a $m/z = [M+Na]^+$ (sodium adduct), ^b $m/z = [M+H]^+$ (protonated ion), ^c Fatty-acid codes: P = palmitic, O = oleic, L = linoleic, S = stearic. Square-bracket notation [Cx:y] denotes the number of carbon atoms (x) and double bonds (y) in the acyl residue. Calculated m/z values were obtained as M(neutral) + 22.9898 (Na⁺) or + 1.0073 (H⁺). Potassium adducts $[M+K]^+ = M + 38.9637$ are omitted from the summary for clarity.

foam collapse after cell opening. Accordingly, suitable surfactants and a precisely adjusted catalytic load are required to ensure that polymer chain elongation proceeds at the optimal rate (Peyrton and Avérous, 2021). For the production of rigid thermal insulation foams, polyols with a high hydroxyl value and functionality are employed (Gama et al., 2018), comparable to the biopolyol synthesized in the present study. As a result, complete (100 %) substitution of the petrochemical polyol with the obtained biopolyols was achieved. Viscoelastic foams, in contrast, are typically manufactured using mixtures of polyols with different characteristics (Auguścik-Królikowska et al., 2021; Nurul 'Ain et al., 2016). In addition to short-chain polyols, long-chain variants with a low hydroxyl value are added to give the final material greater elasticity. The initial formulation of viscoelastic foams was refined through experimentation. The reference foam formulation is a complex composition consisting of three petrochemical polyols: two with a low hydroxyl value of approximately 30 mg KOH/g, and one with a high value of over 400 mg KOH/g. To limit the number of variables, only two of the petrochemical polyols were replaced with a new biopolyol: one with a high hydroxyl value and one with a low hydroxyl value. The polyol with the higher hydroxyl value increases the cross-linking density, while the polyol with the lower hydroxyl value ensures the material's elasticity. Based on our experience, the petrochemical polyol 2 helps achieve stable properties in flexible polyurethane foams. Therefore, a decision was made to keep the amount of this polyol unchanged. The level of the biopolyol additive was determined by previous research, in which biopolyols obtained by a similar method were introduced into viscoelastic foams in amounts ranging from 10 % to 30 % (Malewska et al., 2024b). Using more than 20 % of the biopolyol additive was found to worsen the

properties of viscoelastic foams. The polyurethane systems used to produce viscoelastic foams contain polyols with different chain lengths and hydroxyl values. This makes it easier to achieve unique properties, such as phase separation, and thus prolong the recovery time of the foam material. However, the focus of this article is on the impact of the type of oil used to obtain the biopolyol on the foam properties, rather than on introducing more variable factors. The recipes used to prepare the viscoelastic polyurethane foam and open-cell polyurethane foam are listed in Table 3 and Table 4, respectively. In order to calculate the amount of isocyanate required to react with the polyols, the hydroxyl number, water content of the raw materials and the assumed isocyanate index were taken into account.

By replacing 20 % of the petrochemical polyol with the biopolyols coming from commercial sunflower and from remediation, viscoelastic foams were obtained and subjected to an evaluation of their physical and chemical properties (Fig. 8 and Table 7). The decision to use 20 % of biopolyol in the formulation of viscoelastic foams was based on the authors' previous experience. Further increasing the amount of tri-functional biopolyol would have resulted in excessive cross-linking of the polyurethane material, reduced flexibility and prolonged return time (Malewska et al., 2024b). These properties determine the potential applications of the produced materials.

FTIR analysis of the viscoelastic foam samples (Fig. 8) revealed characteristic urethane bands for all formulations. The absence of the isocyanate stretching band at $\sim 2270\text{ cm}^{-1}$ indicates complete consumption of -NCO groups (Han et al., 2007). A broad band at $3300\text{--}3400\text{ cm}^{-1}$ corresponds to N-H stretching (with overlapping O-H contribution) (Kim et al., 2024), while the strong carbonyl absorption at $\sim 1700\text{--}1730\text{ cm}^{-1}$ (Carriço et al., 2017) and the N-H bending band at $\sim 1510\text{--}1530\text{ cm}^{-1}$ confirm urethane linkage formation (Brzeska et al., 2018). Intense bands in the $1250\text{--}1100\text{ cm}^{-1}$ region are attributed to C-O-C stretches from the polyol segments (Jin et al., 2020). The overall band correspondence suggests that the modifications by BP-C and BP-R did not result in the formation of new, prominently dominant functional groups, and the material retains its polyurethane matrix structure.

The analysis of cell structure and mechanical properties (Table 8) showed that the reference foam has an apparent density of 80 kg/m^3 , which is by about 10 kg/m^3 lower than that of the foams modified with the biopolyols from sunflower oils.

In addition, it was observed that the biopolyol-modified foams, despite their higher apparent density, are characterized by lower hardness, i.e. compressive strength at 40 % strain, which for the modified foams is about 11 kPa, while for the reference foam - 13 kPa. The lower hardness of the modified foams may be related to a change in the composition of the pre-mix, in which part of the branched-chain polyol used to produce rigid polyurethane foams, i.e. polyol 1, was replaced by biopolyol. Although the biopolyol has a similar hydroxyl number, it has in its structure the so-called dangling chains, which can have a plasticizing effect on the polyurethane matrix (Petrovic, 2008). All foams, based on their resilience, can be classified as viscoelastic foams, bearing a bounce of less than 10 % (Polyurethane Foam Association, 2016). Another characteristic property indicating viscoelasticity and the ability to absorb energy is hysteresis. Hysteresis loop diagrams for individual foams are shown in Fig. 9.

It was observed that the reference foam has a lower hysteresis value of 0.87, compared to the foams with the biopolyol, for which the hysteresis is above 0.92. The differences between the foams can be observed in the hysteresis graphs, but they are not significant (Fig. 9). No major differences in physical-mechanical properties were observed across the foams modified with different biopolyols, which is due to the fact that the biopolyols also had similar properties despite the different base material. The return time, which is typically prolonged for viscoelastic foams in contrast to typical conventional elastic foams, was also analyzed. The return time was in the range from 70 to 90 s. The observations confirm that it is possible to successfully replace 20 % of a petrochemical polyol with a sunflower polyol and produce materials

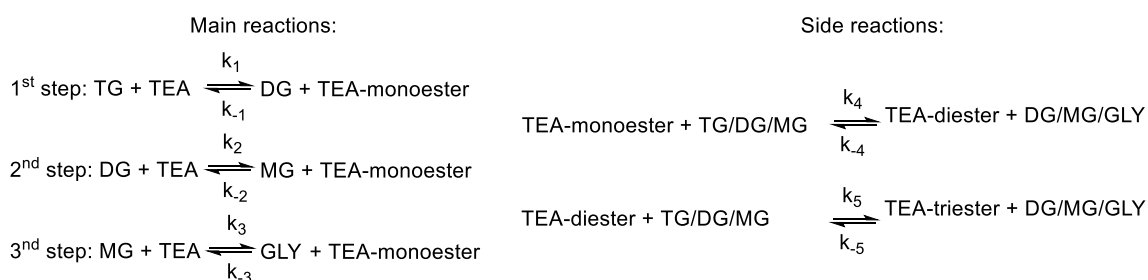
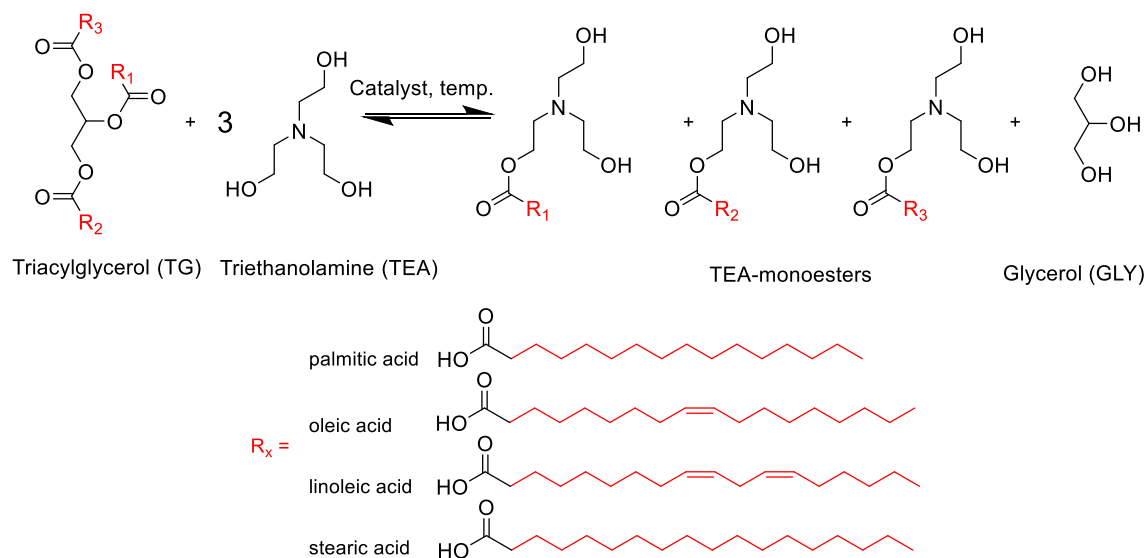


Fig. 6. Reaction scheme illustrating the formation of TEA-based biopolyol, including the generation of intermediate and side products.

Table 6

Characteristics of sunflower oils and biopolyols.

| | Pressing efficiency, % | Mn, g/mol | % H ₂ O, % | Viscosity, mPa·s | OH _{val} , mgKOH/g | Functionality (f _{NMR}) |
|------|------------------------|-----------|-----------------------|------------------|-----------------------------|-----------------------------------|
| O-C | 28 | 880 | 0.14 ± 0.02 | 60 ± 1.2 | - | - |
| O-R | 41 | 890 | 0.12 ± 0.01 | 50 ± 3.1 | - | - |
| BP-C | - | 500 | 0.24 ± 0.00 | 170 ± 5.2 | 329 ± 6.6 | 2.03 ± 0.10 |
| BP-R | - | 500 | 0.36 ± 0.01 | 160 ± 1.9 | 337 ± 4.2 | 1.94 ± 0.04 |

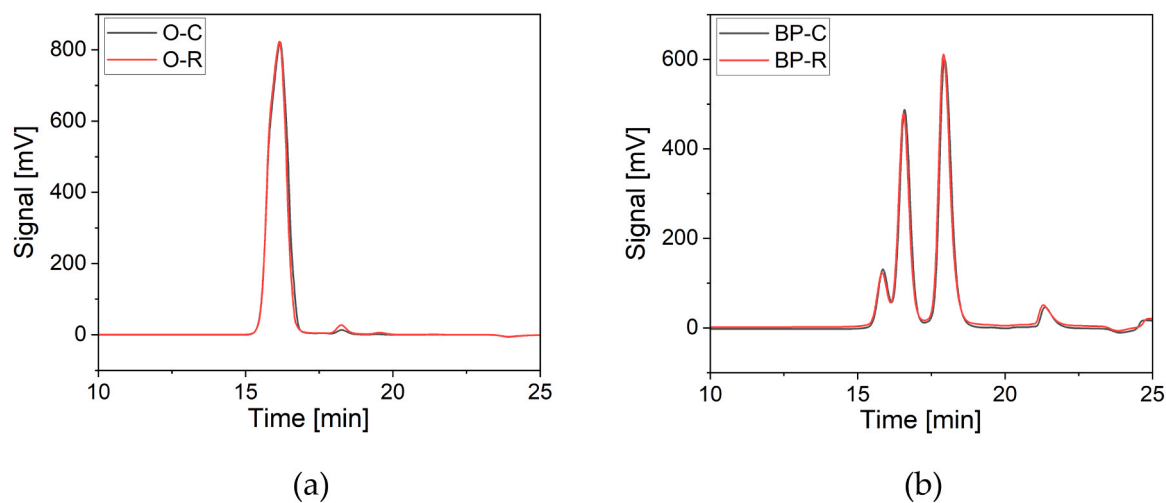


Fig. 7. Chromatograms of (a) oils and (b) biopolyols.

Table 7

Molar masses and peak area contributions of individual peaks for oils and biopolyols.

| | Max. retention time | | | | | | | |
|------|---------------------|--------------|-----------|--------------|-----------|--------------|-----------|--------------|
| | 16' | | 17' | | 18' | | 21' | |
| | Mn, g/mol | Peak area, % | Mn, g/mol | Peak area, % | Mn, g/mol | Peak area, % | Mn, g/mol | Peak area, % |
| O-C | 880 | 100 | - | - | - | - | - | - |
| O-R | 890 | 100 | - | - | - | - | - | - |
| BP-C | 960 | 9.2 | 740 | 37.4 | 455 | 49.8 | 135 | 3.6 |
| BP-R | 970 | 8.5 | 745 | 36.5 | 455 | 50.9 | 140 | 4.1 |

with comparable properties. What is more, a biopolyol derived from commercial sunflower can be replaced by a biopolyol derived from waste sunflower oil obtained from contaminated land remediation.

An additional critical characteristic of polyurethane foams, which can significantly affect their properties and quality, is their cellular structure. Fig. 10 illustrates SEM micrographs of representative cellular structures of viscoelastic polyurethane foams, accompanied by a detailed morphological analysis. The addition of biopolyols was found to influence the cellular structure of the resulting foams, promoting a higher cell density with reduced cell size. The formation of a finer cellular structure is considered beneficial from an application perspective. Literature has reported that biopolyols derived from vegetable oils can function as surfactants, thereby positively affecting foam morphology (Olszewski et al., 2024; Prociak et al., 2021).

The next stage of the research was to obtain samples of open-cell foams that could be used as loft insulation. The foams were obtained according to the formulas given in Table 4. It is noteworthy that the reference foam was made from a 100 % petrochemical polyol, which was entirely replaced by biopolyols in the modified foams. The FTIR spectrum of open-cell thermal insulation polyurethane foams is presented in Fig. 11.

The FTIR spectra of the reference and bio-based polyurethane open-cell foams (OPU-REF, OPU-BP-C, OPU-BP-R) exhibit the characteristic absorption bands of polyurethane materials. The broad band at $\sim 3300\text{ cm}^{-1}$ corresponds to N-H stretching vibrations, while the peaks

at $2800\text{--}3000\text{ cm}^{-1}$ are assigned to C-H stretching. The strong absorption at $\sim 1720\text{ cm}^{-1}$ is attributed to C=O stretching (urethane linkage), accompanied by bands at $1500\text{--}1600\text{ cm}^{-1}$ (N-H bending and C-N stretching) and $1050\text{--}1150\text{ cm}^{-1}$ (C-O-C stretching). Small bands observed at $\sim 2270\text{ cm}^{-1}$ indicate the presence of unreacted isocyanate groups, which results from using an isocyanate index greater than 100 %, i.e., an excess of isocyanate relative to the hydroxyl groups. The spectra of all foams are highly comparable, indicating that the incorporation of biopolyols did not introduce new dominant functional groups.

The properties of open-cell polyurethane foams are presented in Table 9. Properties of rigid polyurethane foams depend significantly on their apparent density. The apparent density affects, among other things, mechanical properties, thermal insulation properties and dimensional stability. The apparent densities of the foam materials obtained in this work are all in the range of $13.3\text{--}15.3\text{ kg/m}^3$. The apparent density of commercially available open-cell foams is approx. $8\text{--}15\text{ kg/m}^3$ (Stefano et al., 2013).

The thermal conductivity for all systems was comparable. The mechanical properties of foam materials mainly depend on the apparent density, cell structure and the chemical structure of the PUR matrix. The compressive strength of the PUR foams studied here was tested in directions perpendicular and parallel to the direction of foam growth at

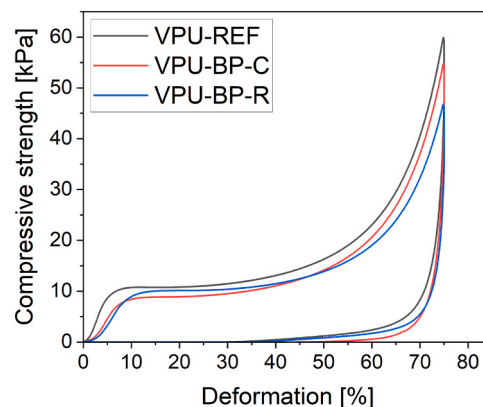


Fig. 9. Hysteresis loops of polyurethane foams modified with biopolyols and reference foam.

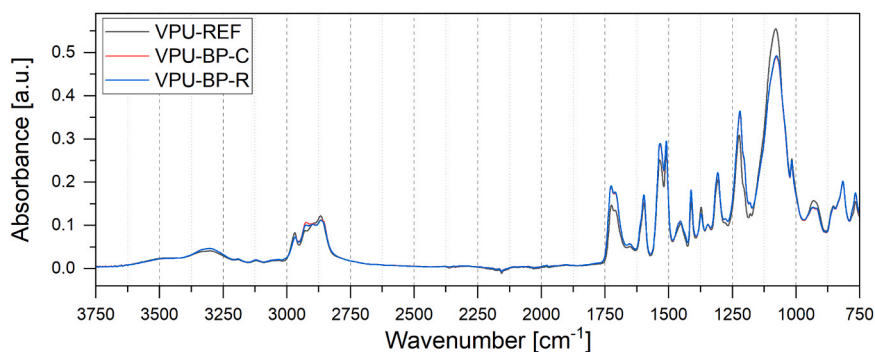


Fig. 8. FTIR spectra of viscoelastic polyurethane foams.

Table 8

Cell structure analysis and physical-mechanical properties of viscoelastic foams containing biopolyols from sunflower seeds and reference foam.

| | Apparent density, kg/m^3 | Hardness, kPa | Resilience, % | Hysteresis | Recovery time, s | Number of cell, cell/mm ² | Cell area, mm ² |
|----------|-----------------------------------|---------------|---------------|-----------------|------------------|--------------------------------------|----------------------------|
| VPU-REF | 79 ± 2.1 | 13 ± 0.5 | < 10 | 0.87 ± 0.00 | 75 ± 5 | 3.35 | 0.223 |
| VPU-BP-C | 91 ± 0.7 | 11 ± 0.8 | < 10 | 0.92 ± 0.01 | 88 ± 10 | 6.60 | 0.107 |
| VPU-BP-R | 93 ± 1.5 | 11 ± 0.3 | < 10 | 0.90 ± 0.01 | 71 ± 8 | 6.71 | 0.111 |

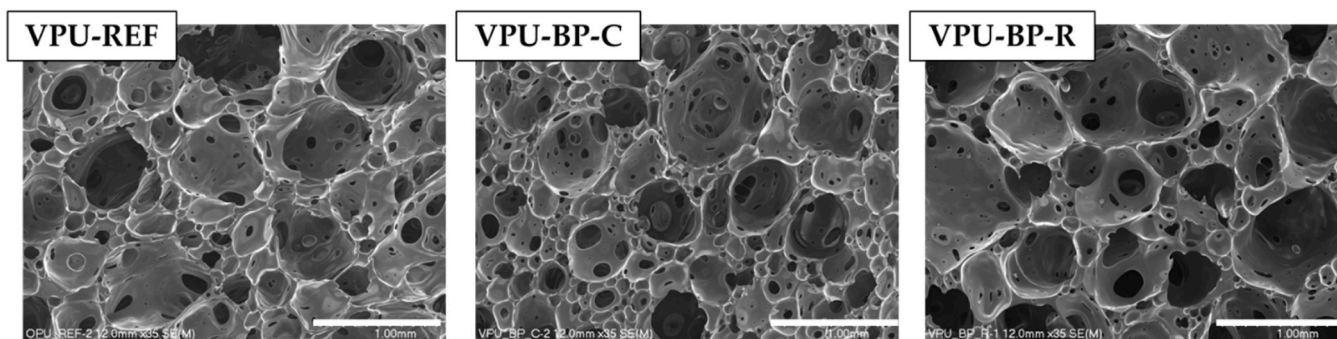


Fig. 10. SEM micrographs (scale bar: 1 mm) of viscoelastic foams.

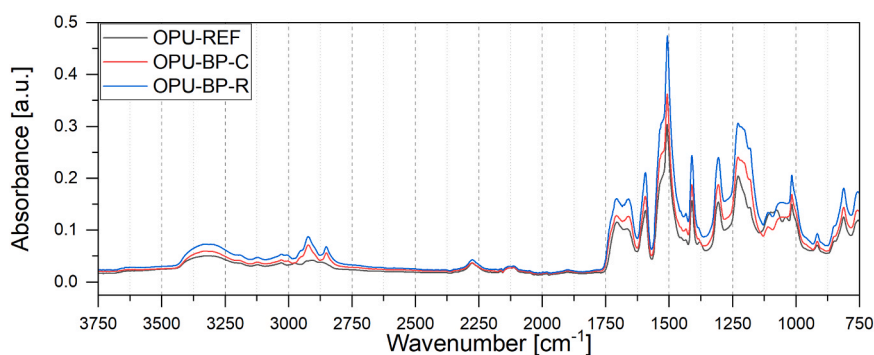


Fig. 11. FTIR spectra of thermal insulation open-cell polyurethane foams.

Table 9

Properties of open-cell polyurethane foams for thermal insulation.

| | Apparent density, kg/ m ³ | Closed cell content, % | Thermal conductivity coefficient, mW/ (m·K) | Compressive strength, kPa | | Number of cell, cell/ mm ² | Cell area, mm ² |
|----------|---|---------------------------|--|---------------------------|----------|--|-------------------------------|
| | | | | | ⊥ | | |
| OPU-REF | 15.3 ± 0.46 | < 5 % | 37.2 ± 0.47 | 69 ± 3.2 | 29 ± 1.3 | 5.03 | 0.173 |
| OPU-BP-C | 13.3 ± 0.77 | < 5 % | 39.2 ± 0.69 | 62 ± 2.5 | 23 ± 3.8 | 6.60 | 0.127 |
| OPU-BP-R | 13.4 ± 0.14 | < 5 % | 38.7 ± 1.19 | 61 ± 2.2 | 23 ± 1.9 | 6.29 | 0.130 |

|| - Compressive strength in the direction parallel to the foam rise; ⊥ - Compressive strength in the direction perpendicular to the foam rise

10 % relative strain at a temperature of about 21°C. The compressive strength of the materials obtained varied with the direction of testing as expected given the anisotropic nature of the cell structure of the foams. The compressive strength found in a perpendicular direction was the highest for the foam OPU-REF (~29 kPa), while it was lower for the foams obtained using biopolyols (~23 kPa). The strength values measured in a parallel direction were higher (~69 kPa for the reference foam and ~62 kPa for the modified foams). The lower compressive strength value of the biofoams could be explained by the plasticizing effect of the biopolyols and lower apparent densities of the foams. It is worth noting that in the open-cell foams discussed here, 100 % of the petrochemical polyol was replaced by a polyol of natural origin. The use of sunflower oil after phytoremediation did not affect the properties of the foams obtained, confirming that oil plants grown for remediation in degraded areas can be a valuable source of raw materials for polyurethane chemistry.

Similarly to the analysis performed for viscoelastic foams, the cellular structure of the foams was examined, and the results are presented in Fig. 12. Once again, it was observed that replacing the petrochemical polyol with a biopolyol derived from sunflower oil led to a reduction in cell size and an increase in cell number.

4. Conclusions

Sunflowers were irrigated with landfill leachate and used for phytoremediation of contaminated soil. It turned out that sunflower seeds grown on contaminated soils did not contain significant amounts of heavy metals and could be used for oil pressing. Sunflower seeds were pressed and the extracted oil was modified to introduce hydroxyl groups. The biopolyols obtained from the modified oil were found to have properties comparable to those of the biopolyols derived from commercial sunflower seeds. The biopolyols were characterized by a hydroxyl number above 300 mgKOH/g and a viscosity below 200 mPa·s, making them suitable for the production of, e.g., open-cell foams for attic insulation and viscoelastic foams for cushions or mattresses. The foams produced also had properties similar to those of commercially available materials. It was additionally demonstrated that the biopolyols obtained can replace petrochemical polyol entirely (100 %) in open-cell thermal-insulation foams and up to 20 % in viscoelastic foams. It was confirmed that it is possible to use oilseeds from phytoremediation plants as a potential source of raw materials for polyurethane chemistry. Therefore, some of the valuable raw materials that are normally wasted could be recycled.

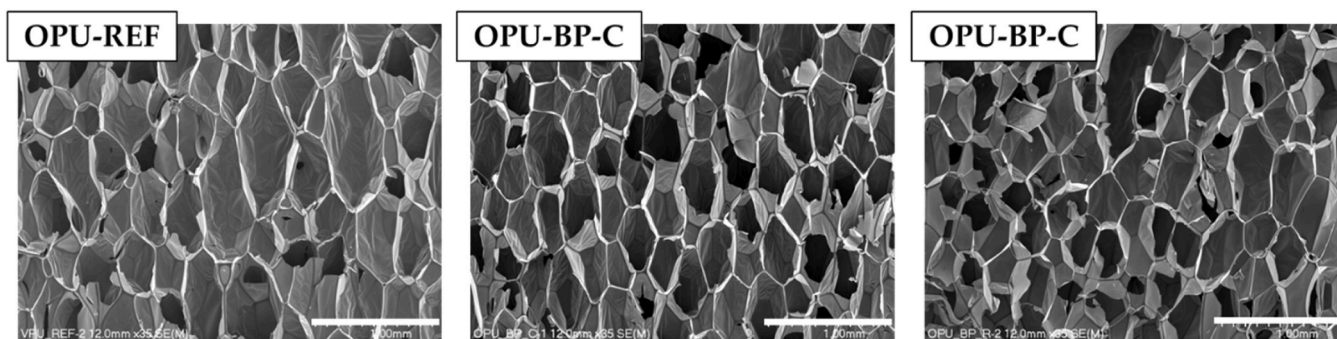


Fig. 12. SEM micrographs of thermal insulation open-cell polyurethane foams.

CRediT authorship contribution statement

Piotr Rybarczyk: Methodology, Investigation. **Maria Kurańska:** Writing – original draft, Methodology, Investigation. **Jacek Antonkiewicz:** Writing – original draft, Supervision, Methodology, Investigation, Conceptualization. **Elżbieta Malewska:** Writing – review & editing, Writing – original draft, Visualization, Methodology, Investigation, Data curation, Conceptualization. **Andrzej Rogala:** Methodology, Investigation.

Funding

This manuscript was prepared within the scope of the Eco-designing for the coastal zone nutrient's circularity (ECONUT) project, co-financed by the EU European Regional Development Fund (ERDF) under the 2021–2027 Interreg VI-A South Baltic cross-border cooperation programme; project number STHB.02.03-IP.01–0004/23, and published as part of an international project co-financed by the program of the Minister of Science and Higher Education entitled “PMW” in 2021–2022-Baltic Phytoremediation (BAPR) under contract no. 5247/SBP 2014–2020/2021/2.

Acknowledgments

The authors are grateful to Bernadetta Boneberger from Evonik Industries AG for supplying a catalyst.

Declaration of Competing Interest

The authors declare the following financial interests/personal relationships which may be considered as potential competing interests: Jacek Antonkiewicz reports financial support was provided by Ministry of Education and Science of the Republic of Poland. If there are other authors, they declare that they have no known competing financial interests or personal relationships that could have appeared to influence the work reported in this paper.

Data availability

The data presented in this study are available on request from the corresponding author.

References

- Adeoye, A.O., Adebayo, I.A., Afodun, A.M., Ajijolakewu, K.A., 2022. Benefits and limitations of phytoremediation: Heavy metal remediation review. *Phytoremediat. Biotechnol. Strateg. Promot. Invigorating Environ* 227–238. <https://doi.org/10.1016/B978-0-323-89874-4.00002-9>.
- Alexandri, E., Ahmed, R., Siddiqui, H., Choudhary, M.I., Tsiakoulis, C.G., Gerothanassis, I.P., 2017. High resolution NMR spectroscopy as a structural and analytical tool for unsaturated lipids in solution. *Molecules* 22. <https://doi.org/10.3390/molecules22101663>.

- Anastopoulos, I., Ighalo, J.O., Adaobi Igwegbe, C., Giannakoudakis, D.A., Triantafyllidis, K.S., Pashalidis, I., Kalderis, D., 2021. Sunflower-biomass derived adsorbents for toxic/heavy metals removal from (waste) water. *J. Mol. Liq.* 342, 117540. <https://doi.org/10.1016/j.molliq.2021.117540>.
- Arthur, E.L., Rice, Pamela J., Rice, Patricia J., Anderson, T.A., Baladi, S.M., Henderson, K.L.D., Coats, J.R., 2005. Phytoremediation - an overview. *CRC. Crit. Rev. Plant Sci.* 24, 109–122. <https://doi.org/10.1080/07352680590952496>.
- Auguścik-Królikowska, M., Ryszkowska, J., Kurańska, M., Wantulok, M., Gloc, M., Szczepkowski, L., Dąbkowska-Suszał, K., Prociak, A., 2021. Composites of open-cell viscoelastic foams with blackcurrant pomace. *Materials* 14, 1–22. <https://doi.org/10.3390/ma14040934>.
- Bashir, S., Qayyum, M.A., Husain, A., Bakhsh, A., Ahmed, N., Hussain, M.B., Elshikh, M. S., Alwahibi, M.S., Almunqedhi, B.M.A., Hussain, R., Wang, Y.F., Zhou, Y., Diao, Z. H., 2021. Efficiency of different types of biochars to mitigate Cd stress and growth of sunflower (*Helianthus; L.*) in wastewater irrigated agricultural soil. *Saudi J. Biol. Sci.* 28, 2453–2459. <https://doi.org/10.1016/j.sjbs.2021.01.045>.
- Borowicz, M., Paciork-Sadowska, J., Isbrandt, M., 2025. From seed to product” – Synthesis of high-value bio-polyol raw materials from white mustard seed processing and assessment of the influence of the degree of oxidation on the properties of the obtained products. *Ind. Crops Prod.* 227, 120813. <https://doi.org/10.1016/j.indcrop.2025.120813>.
- Brzeska, J., Elert, A.M., Morawska, M., Sikorska, W., Kowalczyk, M., Rutkowska, M., 2018. Branched polyurethanes based on synthetic polyhydroxybutyrate with tunable structure and properties. *Polymers* 10, 1–12. <https://doi.org/10.3390/polym10080826>.
- Cakaj, A., Drzewiecka, K., Hanć, A., Lisiak-Zielińska, M., Ciszewska, L., Drapikowska, M., 2024. Plants as effective bioindicators for heavy metal pollution monitoring. *Environ. Res.* 256. <https://doi.org/10.1016/j.envres.2024.119222>.
- Carriço, C.S., Fraga, T., Carvalho, V.E., Pasa, V.M.D., 2017. Polyurethane foams for thermal insulation uses produced from castor oil and crude glycerol biopolysols. *Molecules* 22. <https://doi.org/10.3390/molecules22071091>.
- Cuevas, M.S., Rodrigues, C.E.C., Meirelles, A.J.A., 2009. Effect of solvent hydration and temperature in the deacidification process of sunflower oil using ethanol. *J. Food Eng.* 95, 291–297. <https://doi.org/10.1016/j.jfoodeng.2009.05.009>.
- Di Pietro, M.E., Mannu, A., Mele, A., 2020. NMR determination of free fatty acids in vegetable oils. *Processes* 8. <https://doi.org/10.3390/PR8040410>.
- Dietz, A.C., Schnoor, J.L., 2001. Advances in phytoremediation. *Environ. Health Perspect.* 109, 163–168. <https://doi.org/10.1289/ehp.01109s1163>.
- Fridrihsone-Girone, A., Stirna, U., 2014. Characterization of polyurethane networks based on rapeseed oil derived polyol. *Polim. /Polym.* 59, 333–338. <https://doi.org/10.14314/polimery.2014.333>.
- Gama, N.V., Ferreira, A., Barros-Timmons, A., 2018. Polyurethane foams: past, present, and future. *Polymers*. <https://doi.org/10.3390/polym10101841>.
- Grifoni, M., Pedron, F., Barbaferi, M., Rosellini, I., Petruzzelli, G., Franchi, E., 2021. Sustainable valorization of biomass: from assisted phytoremediation to green energy production. *Handb. Assist. Sustain. Remediat. Technol.* 29–51. <https://doi.org/10.1002/9781119670391.ch2>.
- Han, J.L., Yu, C.H., Lin, Y.H., Hsieh, K.H., 2007. Kinetic study of the urethane and urea reactions of isophorone diisocyanate. *J. Appl. Polym. Sci.* 107, 3891–3902. <https://doi.org/10.1002/app.27421>.
- Ionescu, M., Petrović, Z.S., 2010. High functionality polyether polyols based on polyglycerol. *J. Cell. Plast.* 46, 223–237. <https://doi.org/10.1177/0021955X09355887>.
- Jin, X., Guo, N., You, Z., Tan, Y., 2020. Design and performance of polyurethane elastomers composed with different soft segments. *Materials* 13, 1–26. <https://doi.org/10.3390/ma13214991>.
- Kabata-Pendias, A., 2010. *Trace Elements in Soils and Plants*, 4th ed. CRC Press. Taylor and Francis Group: Boca Raton, FL, USA, 2010; pp. 505.
- Kabata-Pendias, A., Motowicka-Terelak, T., Piotrowska, M., Terelak, H., Witek, T., 1993. Assessment the degree of soil and plant pollution with heavy metals and sulphur. Framework guidelines for agriculture. *In: Pulawy, series P*, 53. IUNG, p. 20. [in Polish].
- Kara, S., Hauschild, M., Sutherland, J., McAlloone, T., 2022. Closed-loop systems to circular economy: a pathway to environmental sustainability? *CIRP Ann.* 71, 505–528. <https://doi.org/10.1016/j.cirp.2022.05.008>.

- Keera, S.T., El Sabagh, S.M., Taman, A.R., 2011. Transesterification of vegetable oil to biodiesel fuel using alkaline catalyst. *Fuel* 90, 42–47. <https://doi.org/10.1016/j.fuel.2010.07.046>.
- Kim, H.J., Jin, X., Choi, J.W., 2024. Investigation of bio-based rigid polyurethane foams synthesized with lignin and castor oil. *Sci. Rep.* 14, 1–13. <https://doi.org/10.1038/s41598-024-64318-8>.
- Kurańska, M., Malewska, E., 2021. Waste cooking oil as starting resource to produce biopolyol - analysis of transesterification process using gel permeation chromatography. *Ind. Crops Prod.* 162, 1–8. <https://doi.org/10.1016/j.indcrop.2021.113294>.
- Kurańska, M., Beneš, H., Salasińska, K., Prociak, A., Malewska, E., Polaczek, K., 2020. Development and characterization of “green open-cell polyurethane foams” with reduced flammability. *Materials* 13, 1–17. <https://doi.org/10.3390/ma13235459>.
- Malewska, E., Polaczek, K., Kurańska, M., 2022. Impact of various catalysts on transesterification of used cooking oil and foaming processes of polyurethane systems. *Materials* 15. <https://doi.org/10.3390/ma15217807>.
- Malewska, E., Prociak, T., Michałowski, S., Barczewski, M., Banaś, J., Kurańska, M., Prociak, A., 2024b. Environmentally friendly shape memory biofoams. *Biomass Convers. Biorefinery*. <https://doi.org/10.1007/s13399-024-06385-5>.
- Malewska, E., Kirpluks, M., Słota, J., Banaś, J., Kurańska, M., 2024a. Open-cell bio-based polyurethane foams modified with biopolyols from non-edible oilseed radish oil. *Clean. Technol. Environ. Policy*. <https://doi.org/10.1007/s10098-024-02740-2>.
- Mondal, M.G., Pratap, A.P., 2016. Synthesis and performance properties of cationic fabric softeners derived from free fatty acid of tallow fat. *J. Oleo Sci.* 65, 663–670. <https://doi.org/10.5650/jos.ess15276>.
- Motuzova, G.V., Minkina, T.M., Karpova, E.A., Barsova, N.U., Mandzhieva, S.S., 2014. Soil contamination with heavy metals as a potential and real risk to the environment. *J. Geochem. Explor.* 144, 241–246. <https://doi.org/10.1016/j.gexplo.2014.01.026>.
- Nakonechna, K., Ilko, V., Berčíková, M., Vietoris, V., Panovská, Z., Doležal, M., 2024. Nutritional, utility, and sensory quality and safety of sunflower oil on the central european market. *Agric* 14, 1–12. <https://doi.org/10.3390/agriculture14040536>.
- Nurul 'Ain, H., Maznee, T.I.T.N., Norhayati, M.N., Noor, M.A.M., Adnan, S., Devi, P.P.K., Norhisham, S.M., Yeong, S.K., Hazimah, A.H., Campara, I., Sendijarevic, V., Sendijarevic, I., 2016. Natural palm olein polyol as a replacement for polyether polyols in viscoelastic polyurethane foam. *JAOS J. Am. Oil Chem. Soc.* 93, 983–993. <https://doi.org/10.1007/s11746-016-2832-7>.
- Ociepa-Kubicka, A., Ociepa, E., 2012. Toksyczne oddziaływanie metali ciężkich na rośliny, zwierzęta i ludzi. *Żywność i Ochr. Środowiska* T 15, 169–180 (nr).
- Olszewski, A., Kosmela, P., Věvere, L., Kirpluks, M., Cabulis, U., Piszczek, Ł., 2024. Effect of bio-polyol molecular weight on the structure and properties of polyurethane-polyisocyanurate (PUR-PIR) foams. *Sci. Rep.* 14, 1–15. <https://doi.org/10.1038/s41598-023-50764-3>.
- Parliament of the Republic of Poland, 2020. *Dziennik ustaw* 1360. *J. Laws Pol.* 1, 10.
- Petrovic, Z.S., 2008. Polyurethanes from vegetable oils. *Polym. Rev.* 48, 109–155. <https://doi.org/10.1080/15583720701834224>.
- Peyrton, J., Avérous, L., 2021. Structure-properties relationships of cellular materials from biobased polyurethane foams. *Mater. Sci. Eng. R. Rep.* 145. <https://doi.org/10.1016/j.mser.2021.100608>.
- Polyurethane Foam Association, 2016. Viscoelastic memory foam. *In-Touch* 11, 1–7.
- Prociak, A., Kurańska, M., Uram, K., Wójtowicz, M., 2021. Bio-polyurethane foams modified with a mixture of bio-polyols of different chemical structures. *Polym. (Basel)* 13. <https://doi.org/10.3390/polym13152469>.
- Qiao, D., Han, Y., Zhao, Y., 2022. Organic acids in conjunction with various oilseed sunflower cultivars promote Cd phytoextraction through regulating micro-environment in root zone. *Ind. Crops Prod.* 183, 114932. <https://doi.org/10.1016/j.indcrop.2022.114932>.
- Sawpan, M.A., 2018. Polyurethanes from vegetable oils and applications: a review. *J. Polym. Res.* 25. <https://doi.org/10.1007/s10965-018-1578-3>.
- da Silva, T.A., Ramos, L.P., Zawadzki, S.F., Barbosa, R.V., 2015. Application of Taguchi design to produce polyols based on castor oil derivatives with diethylene glycol. *Mediterr. J. Chem.* 4, 93–99. <https://doi.org/10.13171/mjc.4.2.2015.11.04.15.35/barbosa>.
- Stefano, F., Alice, L., Georgios, K., Dmytro, L., Gianluca, S., Europe, P., 2013. Closed and open-cell spray polyurethane foam. *Energy Procedia* 441–446.
- Stirna, U., Cabulis, U., Beverte, I., 2008. Water-blown polyisocyanurate foams from vegetable oil polyols. *J. Cell. Plast.* 44, 139–160. <https://doi.org/10.1177/0021955X07084705>.
- Stirna, U., Fridrihsone, A., Lazdiņa, B., Misāne, M., Vilsone, D., 2013. Biobased polyurethanes from rapeseed oil polyols: structure, mechanical and thermal properties. *J. Polym. Environ.* 21, 952–962. <https://doi.org/10.1007/s10924-012-0560-0>.
- Tan, H.W., Pang, Y.L., Lim, S., Chong, W.C., 2023. A state-of-the-art of phytoremediation approach for sustainable management of heavy metals recovery. *Environ. Technol. Innov.* 30, 103043. <https://doi.org/10.1016/j.eti.2023.103043>.
- Tran, M.H., Lee, E.Y., 2023. Production of polyols and polyurethane from biomass: a review. *Environ. Chem. Lett.* 21, 2199–2223. <https://doi.org/10.1007/s10311-023-01592-4>.
- Uddin, M.M., Cassim, M.Z., Zavahir, M., Shezmin, J., 2021. Heavy metal accumulation in rice and aquatic plants used as. *Toxics* 9, 1–19.
- Waseem, M., Khilji, S.A., Tariq, S., Jamal, A., Alomrani, S.O., Javed, T., 2024. Phytoremediation of heavy metals from industrially contaminated soil using sunflower (*Helianthus annuus* L.) by inoculation of two indigenous bacteria. *Plant Stress* 11. <https://doi.org/10.1016/j.stress.2023.100297>.
- Yang, Y., Zhou, X., Tie, B., Peng, L., Li, H., Wang, K., Zeng, Q., 2017. Comparison of three types of oil crop rotation systems for effective use and remediation of heavy metal contaminated agricultural soil. *Chemosphere* 188, 148–156. <https://doi.org/10.1016/j.chemosphere.2017.08.140>.